

Generating double NOON states of photons in circuit QED

Qi-Ping Su¹, Hui-Hao Zhu¹, Li Yu¹, Yu Zhang¹, Shao-Jie Xiong², Jin-Ming Liu², and Chui-Ping Yang^{1*}

¹*Department of Physics, Hangzhou Normal University, Hangzhou, Zhejiang 310036, China and*

²*State Key Laboratory of Precision Spectroscopy, Department of Physics, East China Normal University, Shanghai 200062, China*

(Dated: March 15, 2018)

To generate a NOON state with a large photon number N , the number of operational steps could be large and the fidelity will decrease rapidly with N . Here we propose a method to generate a new type of quantum entangled states, $(|NN00\rangle + |00NN\rangle)/\sqrt{2}$ called “double NOON” states, with a setup of two superconducting flux qutrits and five circuit cavities. This scheme operates essentially by employing a two-photon process, i.e., two photons are simultaneously and separately emitted into two cavities when each coupler qutrit is initially in a higher-energy excited state. As a consequence, the “double” NOON state creation needs only $N+2$ operational steps. One application of double NOON states is to get a phase error of $1/(2N)$ in phase measurement. In comparison, to achieve the same error, a normal NOON state of the form $(|2N, 0\rangle + |0, 2N\rangle)/\sqrt{2}$ is needed, which requires at least $2N$ operational steps to prepare by using the existing schemes. Our numerical simulation demonstrates that high-fidelity generation of the double NOON states with $N \leq 10$ even for the imperfect devices is feasible with the present circuit QED technique.

PACS numbers: 03.67.Lx, 42.50.Dv, 85.25.Cp

I. INTRODUCTION

Superconducting qubits have attracted substantial attention because of their controllability, integrability, ready fabrication and potential scalability [1–4] in quantum information and quantum computation. The level spacings of superconducting qubits can be rapidly adjusted ($1 \sim 3$ ns) by varying external control parameters [5–8]. Their coherence time is increasing rapidly [9–14]. The strong coupling and ultrastrong coupling of one qubit with one microwave cavity have been reported in experiments [15, 16]. The circuit QED is considered as one of the most feasible candidates for quantum computation [3, 4].

The NOON states, $(|N0\rangle_{12} + |0N\rangle_{12})/\sqrt{2}$ with N photons in mode 1 or 2, have attracted considerable attention because of their significant applications in quantum optical lithography [17, 18], quantum metrology [19–21], precision measurement [22], and quantum information processing [23]. For example, if a photon in mode 2 gains an extra phase $e^{i\phi}$ compared with a photon in mode 1, the NOON state of N photons will become $(|N0\rangle_{12} + e^{iN\phi}|0N\rangle_{12})/\sqrt{2}$ (a common phase has been ignored). With this state, the measurement of $A_N = (|N0\rangle_{12} + |0N\rangle_{12})(\langle N0|_{12} + \langle 0N|_{12})/2$ gives $\langle A_N \rangle = [1 + \cos(N\phi)]/2$. Note that $A_N^2 = A_N$, one has $(\Delta A_N)^2 = \langle A_N^2 \rangle - \langle A_N \rangle^2 = \sin^2(N\phi)/4$. According to [18], the error in the phase is calculated as:

$$\Delta\phi = \Delta A_N / |d\langle A_N \rangle / d\phi| = 1/N, \quad (1)$$

which reaches the Heisenberg limit $1/\bar{N}$ (\bar{N} is the average number of photons counted in a chosen time interval) [24]. It is obvious that the error of phase measurement will be better for a larger photon number N , but the high-fidelity generation of NOON states with a large N is not easy in experiments.

Some schemes have been presented for the generation of the NOON states, $(|N0\rangle + |0N\rangle)/\sqrt{2}$, of photons in two cavities or resonators. The setup in Ref. [25] consists of two superconducting cavities and a tunable qubit, and the qubit alternatively interacts with two cavity modes and a classical pulse respectively. According to [25], generating a NOON state requires a linear number of operations, which is greater than N (e.g., 12 basic operations required for creating a NOON state with $N = 3$). The circuit in Ref. [26] is more complicated, which requires three superconducting resonators and two qutrits, but only $N + 1$ operational steps are needed. The scheme presented in Ref. [26] has been implemented in experiments to generate a NOON state with $N \leq 3$ [27]. Ref. [28] adopts a setup consisting of one superconducting transmon qutrit and two resonators, which is simpler than that in Refs. [26, 27]. Though $2N$ steps of operation are required to generate a NOON state with N photons, the generation of NOON

*Electronic address: yangcp@hznu.edu.cn

states in this scheme is faster than that in Ref. [25]. Then, the scheme in Ref. [28] is improved in Ref. [29], in which one four-level superconducting flux device and two resonators are required while only $N + 1$ operational steps are needed. From the discussion given here, one can see that by using schemes [25-29] to generate a NOON state $(|N0\rangle + |0N\rangle)/\sqrt{2}$ of photons, at least N operational steps are needed.

In this paper, we propose an efficient scheme for generating the ‘‘double’’ NOON states $(|NN00\rangle + |00NN\rangle)/\sqrt{2}$ in four cavities or resonators with only $N + 2$ operational steps (including two basic steps for initial preparation of a two-qutrit Bell state). The setup consists of two superconducting flux qutrits and five cavities (see Fig. 2). A two-photon process is adopted in this scheme, which is quite different from the single-photon process used in Ref. [25–29]. It is the first time to demonstrate that a double NOON state, a new type of NOON states of photons, can be generated in cavity/circuit QED.

For the concrete use of the double NOON states, let us consider their application in phase measurement, which can be implemented by using a setup illustrated in Appendix. Assume that photons in four modes (1, 2, 3, 4) are initially in a double NOON state $(|NN00\rangle_{1234} + |00NN\rangle_{1234})/\sqrt{2}$. Each photon in mode 3 (4) experiences an extra phase shift ϕ compared to each photon in mode 1 (2), which is induced by a phase shifter. When the photons reach their detectors, the double NOON state of photons in four modes (1, 2, 3, 4) can thus be expressed as $|\Psi\rangle = (|NN00\rangle_{1234} + e^{i2N\phi}|00NN\rangle_{1234})/\sqrt{2}$ (a common phase has been ignored). The measurement of $A_{DN} = (|NN00\rangle_{1234} + |00NN\rangle_{1234})(\langle NN00|_{1234} + \langle 00NN|_{1234})/2$ gives:

$$\langle A_{DN} \rangle = \langle \Psi | \cdot A_{DN} \cdot | \Psi \rangle = [1 + \cos(2N\phi)]/2. \quad (2)$$

In addition, one has $(\Delta A_{DN})^2 = \frac{1}{4} \sin^2(2N\phi)$. Thus, the error of phase measurement will be $\Delta\phi = 1/(2N)$, which also reaches the Heisenberg limit. In comparison, to achieve the same error for phase measurement, a normal NOON state of the form $(|2N, 0\rangle + |0, 2N\rangle)/\sqrt{2}$ is needed, which requires at least $2N$ operational steps to prepare by using the existing schemes [25-29].

This paper is arranged as follows. In Sec. II, we introduce the effective Hamiltonian and time evolution for the left-hand half as well as the right-hand half of the setup [Fig. 2(a)]. In Sec. III, we describe how to generate the double NOON states of photons in four cavities or resonators. In Sec. IV, we discuss the possible experimental implementation of this proposal.

II. EFFECTIVE HAMILTONIAN AND TIME EVOLUTION

The setup, shown in Fig. 1(a), consists of two superconducting flux qutrits and five cavities. In Fig. 1(a), the left-hand qutrit is labelled as qutrit L while the right-hand qutrit is labelled as qutrit R . Qutrit L is coupled to cavities 1 and 2 while qutrit R is coupled to cavities 3 and 4. In addition, both qutrits L and R are connected by a common central cavity. Each qutrit has three energy levels $|g\rangle$, $|e\rangle$, and $|f\rangle$. In the following, we first introduce the effective Hamiltonian and time evolution for the left-hand half of the setup (i.e., qutrit L and cavities 1 and 2). We then introduce the effective Hamiltonian and time evolution for the right-hand half of the setup (i.e., qutrit R and cavities 3 and 4).

Suppose that cavity 1 (2) is coupled to the $|g\rangle \leftrightarrow |e\rangle$ ($|e\rangle \leftrightarrow |f\rangle$) transition of the coupler qutrit L . In the interaction picture, the Hamiltonian describing the interaction between qutrit L and the two cavities 1 and 2 is (assuming $\hbar = 1$)

$$H_I(a_1, a_2) = g_1(e^{i\delta_1 t} a_1 \sigma_{ge,L}^+ + h.c.) + g_2(e^{-i\delta_2 t} a_2 \sigma_{ef,L}^+ + h.c.), \quad (3)$$

where $\delta_1 = \omega_{ge,L} - \omega_{c1} > 0$, $\delta_2 = \omega_{c2} - \omega_{ef,L} > 0$, ω_{ge} (ω_{ef}) is the $|g\rangle \leftrightarrow |e\rangle$ ($|e\rangle \leftrightarrow |f\rangle$) transition frequency, ω_{c1} (ω_{c2}) is the frequency of cavity 1 (2), and g_1 (g_2) is the coupling strength between cavity 1 (2) and the $|g\rangle \leftrightarrow |e\rangle$ ($|e\rangle \leftrightarrow |f\rangle$) transition [Fig. 1(b)]. In addition, $\sigma_{ge,L}^+ = |e\rangle_L \langle g|$, $\sigma_{ef,L}^+ = |f\rangle_L \langle e|$, and a_1 (a_2) is the photon annihilation operator of cavity 1 (2).

Under the large-detuning condition $\delta_1 \gg g_1$ and $\delta_2 \gg g_2$, the dynamics governed by $H_I(a_1, a_2)$ is equivalent to that decided by the following effective Hamiltonian [30]

$$H_{eff} = H_0 + H_{int}, \quad (4)$$

with

$$H_0 = -\frac{g_1^2}{\delta_1} (a_1^\dagger a_1 |g\rangle_L \langle g| - a_1 a_1^\dagger |e\rangle_L \langle e|) - \frac{g_2^2}{\delta_2} (a_2 a_2^\dagger |f\rangle_L \langle f| - a_2^\dagger a_2 |e\rangle_L \langle e|), \quad (5)$$

$$H_{int} = -\lambda \left[e^{-i(\delta_1 - \delta_2)t} a_1^\dagger a_2^\dagger |g\rangle_L \langle f| + h.c. \right], \quad (6)$$

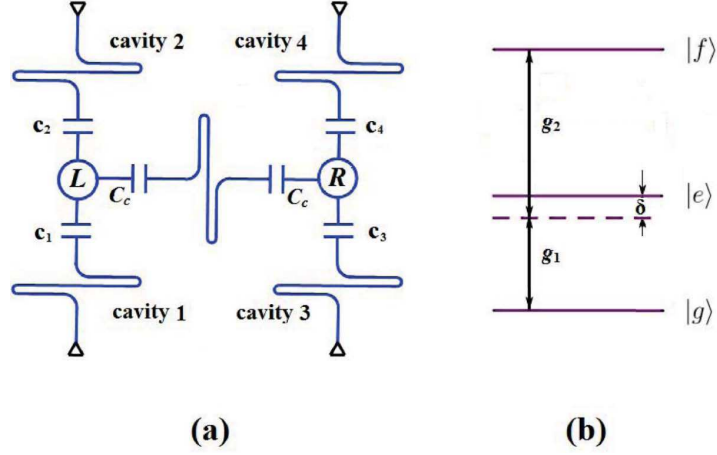


FIG. 1: (Color online) (a) Setup for two superconducting flux qutrits and five cavities. A common cavity (i.e., the central one) is used to initially prepare the two qutrits in a Bell state, while the other four cavities are utilized to create the double NOON state. Here, each cavity is a one-dimensional transmission line resonator. The left-hand circle represents the qutrit labeled by L ; while the right-hand circle represents the qutrit labeled by R . (b) Illustration of each qutrit dispersively interacting with its two cavities. Here, g_1 is the coupling strength between cavity 1 (3) with the $|g\rangle \leftrightarrow |e\rangle$ while g_2 is the coupling strength between cavity 2 (4) with the $|e\rangle \leftrightarrow |f\rangle$ transition. In addition, we set $\delta_1 = \delta_2 = \delta$.

where $\lambda = \frac{g_1 g_2}{2} \left(\frac{1}{\delta_1} + \frac{1}{\delta_2} \right)$. In a new interaction picture with respect to the free Hamiltonian H_0 , one has

$$\begin{aligned} \tilde{H}_{int} &= e^{iH_0 t} H_{int} e^{-iH_0 t} \\ &= -\lambda \left[e^{-i(\delta_1 - \delta_2)t} e^{-i\frac{g_1^2}{\delta_1} a_1^+ a_1 t} a_1^+ a_2^+ |g\rangle_L \langle f| e^{i\frac{g_2^2}{\delta_2} a_2 a_2^+ t} + h.c. \right]. \end{aligned} \quad (7)$$

Denote $|n\rangle_j$ as the n -photon state for cavity j ($j = 1, 2$). Under the Hamiltonian (7), the state $|f\rangle_L |n\rangle_1 |n\rangle_2$ evolves in a subspace formed by two orthogonal states $|f\rangle_L |n\rangle_1 |n\rangle_2$ and $|g\rangle_L |n+1\rangle_1 |n+1\rangle_2$. In this subspace, the Hamiltonian (7) can be expressed as

$$\tilde{H}_{int} = \begin{pmatrix} 0 & -e^{i(\delta_1 - \delta_2)t} e^{i\varphi(n+1)t} (n+1)\lambda \\ -e^{-i(\delta_1 - \delta_2)t} e^{-i\varphi(n+1)t} (n+1)\lambda & 0 \end{pmatrix}, \quad (8)$$

where $\varphi = g_1^2/\delta_1 - g_2^2/\delta_2$. To make the Hamiltonian (8) time independent, the conditions $\delta_1 = \delta_2$ and $g_1 = g_2$ (i.e., $\varphi = 0$) need to be satisfied. Note that $\delta_1 = \delta_2$ can be met by adjusting the level spacings of the qutrit or the cavity frequency, and $g_1 = g_2$ can be achieved by a prior design of the sample with appropriate capacitances c_1 and c_2 . Under the conditions $\delta_1 = \delta_2 \equiv \delta$ and $g_1 = g_2 \equiv g$, the matrix (8) becomes

$$\tilde{H}_{int} = \begin{pmatrix} 0 & -(n+1)\lambda \\ -(n+1)\lambda & 0 \end{pmatrix}, \quad (9)$$

where $\lambda = g^2/\delta$ (which will apply below). Under the Hamiltonian (9), the time evolution of the state $|f\rangle_L |n\rangle_1 |n\rangle_2$ can be described as

$$|f\rangle_L |n\rangle_1 |n\rangle_2 \rightarrow \cos[(n+1)\lambda t] |f\rangle_L |n\rangle_1 |n\rangle_2 + i \sin[(n+1)\lambda t] |g\rangle_L |n+1\rangle_1 |n+1\rangle_2. \quad (10)$$

We now return to the original interaction picture by applying a unitary transformation $e^{-iH_0 t}$ to the right side of Eq. (10). It can be found that in the original interaction picture, the state transformation (10) becomes

$$|f\rangle_L |n\rangle_1 |n\rangle_2 \rightarrow e^{i(n+1)\lambda t} \{ \cos[(n+1)\lambda t] |f\rangle_L |n\rangle_1 |n\rangle_2 + i \sin[(n+1)\lambda t] |g\rangle_L |n+1\rangle_1 |n+1\rangle_2 \}. \quad (11)$$

On the other hand, one can easily find that under the effective Hamiltonian (4), the state $|e\rangle|0\rangle|0\rangle$ evolves into

$$|e\rangle_L |0\rangle_1 |0\rangle_2 \rightarrow e^{-i\lambda t} |e\rangle_L |0\rangle_1 |0\rangle_2. \quad (12)$$

Note that the right-hand half of the setup in Fig. 1(a) has the same configuration as the left-hand half. Therefore, for qutrit R being identical to qutrit L and cavity 3 (4) identical to cavity 1 (2), the Hamiltonian describing the right-hand half of Fig. 2(a) would be

$$H_I(a_3, a_4) = \hbar g_1(e^{i\delta t} a_3 \sigma_{ge,R}^+ + h.c.) + \hbar g_2(e^{-i\delta t} a_4 \sigma_{ef,R}^+ + h.c.), \quad (13)$$

where $\sigma_{ge,R}^+ = |e\rangle_R \langle g|$, $\sigma_{ef,R}^+ = |f\rangle_R \langle e|$. Note that this Hamiltonian takes the same form as the Hamiltonian (3) above. Thus, the state evolution for the coupler qutrit R and cavities 3 and 4 would be the same as those given in Eqs. (11) and (12), with a replacement of the subscripts $L, 1, 2$ by $R, 3, 4$. Namely, under the Hamiltonian (13), we have the following state evolutions

$$|f\rangle_R |n\rangle_3 |n\rangle_4 \rightarrow e^{i(n+1)\lambda t} \{ \cos[(n+1)\lambda t] |f\rangle_R |n\rangle_3 |n\rangle_4 + i \sin[(n+1)\lambda t] |g\rangle_R |n+1\rangle_3 |n+1\rangle_4 \}, \quad (14)$$

$$|e\rangle_R |0\rangle_3 |0\rangle_4 \rightarrow e^{-i\lambda t} |e\rangle_R |0\rangle_3 |0\rangle_4. \quad (15)$$

The results (11), (12), (14) and (15) obtained here will be employed for the preparation of the “double” NOON state below.

As shown in the next section, the double NOON state preparation employs the same operations simultaneously performed on the left-hand two cavities and the right-hand two cavities. Thus, the combined interaction Hamiltonian would be

$$H_{I,1} = H_I(a_1, a_2) + H_I(a_3, a_4), \quad (16)$$

where $H_I(a_1, a_2)$ and $H_I(a_3, a_4)$ commute with each other.

III. PREPARATION OF THE TWO-QUTRIT BELL STATE

Each qutrit is initially decoupled from its connected cavities, which can be achieved by a prior adjustment of the qutrit level spacings via varying external control parameters [1, 31]. In addition, assume that the central cavity is initially in a single-photon state and each qutrit is initially in the ground state $|g\rangle$.

The Bell state of the two qutrits L and R is generated via the following operations:

Adjust the level spacings of the qutrits such that the $|g\rangle \leftrightarrow |e\rangle$ transition of each qutrit is resonant with the central cavity but each qutrit is decoupled from other cavities. In the interaction picture (the same picture is used without mentioning hereafter), the interaction Hamiltonian describing this operation is $h_I = \sum_{j=L,R} \mu_j (a^\dagger \sigma_{ge,j}^- + h.c.)$, where a^\dagger is the photon creation operator for the central cavity, μ_j is the coupling strength between the central cavity and the $|g\rangle \leftrightarrow |e\rangle$ transition of qutrit j , and $\sigma_{ge,j}^- = |g\rangle_j \langle e|$ ($j = L, R$). For simplicity, we assume $\mu_1 = \mu_2 = \mu$, which applies for identical qutrits L and R . It is straightforward to show that the time evolution of the state $|g\rangle |g\rangle |1\rangle$ under the Hamiltonian h_I is described by $|g\rangle |g\rangle |1\rangle \rightarrow \cos(\sqrt{2}\mu t) |g\rangle |g\rangle |1\rangle - \frac{i}{\sqrt{2}} \sin(\sqrt{2}\mu t) (|e\rangle |g\rangle + |g\rangle |e\rangle) |0\rangle$. Here, $|0\rangle$ and $|1\rangle$ are the vacuum state and the single-photon state of the central cavity, respectively. In addition, $|k\rangle |l\rangle \equiv |k\rangle_L |l\rangle_R$ with $k, l \in \{g, e, f\}$ (Here and below, for simplicity we omit the subscripts L and R). One can see that after an interaction time $\tau = \pi / (2\sqrt{2}\mu)$, the initial state $|g\rangle |g\rangle |1\rangle$ of the two qutrits plus the central cavity evolves to

$$\frac{1}{\sqrt{2}} (|g\rangle |e\rangle + |e\rangle |g\rangle) |0\rangle, \quad (17)$$

where a common phase factor $-i$ is omitted. Eq. (17) shows that the two qutrits are prepared in the Bell state while the central cavity is in the vacuum state after the operations. The level spacings of the qutrits need to be adjusted back to the original level configuration such that the qutrits are decoupled from the central cavity.

Note that during the operations described below for the double NOON state creation, the central cavity is not involved. Thus, the central cavity can be dropped off for simplicity.

IV. GENERATION OF THE DOUBLE NOON STATES

Similar to the NOON state preparation, the double NOON state creation requires applying classical pulses. For simplicity, we define ω_{gf} (ω_{ge}) as the $|g\rangle \leftrightarrow |f\rangle$ ($|g\rangle \leftrightarrow |e\rangle$) transition frequency of the qutrits, and define Ω_{gf} (Ω_{ge}) as the Rabi frequency of a classical pulse driving $|g\rangle \leftrightarrow |f\rangle$ ($|g\rangle \leftrightarrow |e\rangle$) transition of the qutrits. The frequency, duration, and initial phase of the pulses are denoted as $\{\omega, t, \varphi\}$.

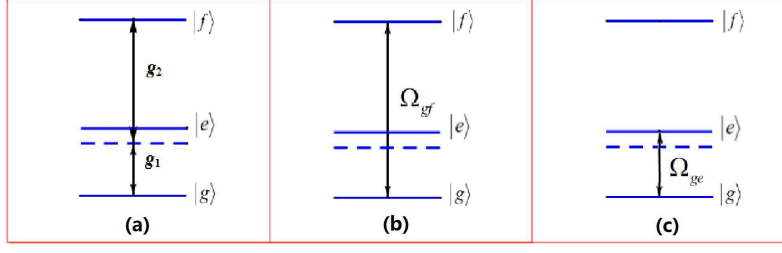


FIG. 2: (Color online) (a) Illustration of the dispersive interaction of qutrit L (R) with cavities 1 and 2 (3 and 4). g_1 is the coupling constant between cavity 1 (3) and the $|g\rangle \leftrightarrow |e\rangle$ transition of qutrit L (R), and g_2 is the coupling constant between cavity 2 (4) and the $|e\rangle \leftrightarrow |f\rangle$ transition of qutrit L (R). (b) Illustration of the resonant interaction between the pulse and the $|g\rangle \leftrightarrow |f\rangle$ transition of each qutrit with the Rabi frequency Ω_{gf} . (c) Illustration of the resonant interaction between the pulse and the $|g\rangle \leftrightarrow |e\rangle$ transition of each qutrit with the Rabi frequency Ω_{ge} .

Assume that each side cavity is initially in the vacuum state and the two qutrits are initially prepared in the Bell state. Thus, the state of the two qutrits and the four side cavities is

$$\frac{1}{\sqrt{2}}(|g\rangle|e\rangle + |e\rangle|g\rangle)|0\rangle_1|0\rangle_2|0\rangle_3|0\rangle_4, \quad (18)$$

where the subscripts 1, 2, 3, and 4 indicate the four cavities 1, 2, 3, and 4, respectively.

Before starting the double NOON state preparation, a classical pulse of $\{\omega_{gf}, \frac{\pi}{2\Omega_{gf}}, -\frac{\pi}{2}\}$ needs to be applied to the qutrits [Fig. 2(b)], which is described by the following Hamiltonian

$$H_{I,2} = \sum_{j=L,R} (\Omega_{gf} e^{i\pi/2} \sigma_{gf,j}^+ + h.c.), \quad (19)$$

where $\sigma_{gf,j}^+ = |f\rangle_j \langle g|$. It is easy to find that under the Hamiltonian (19), we have the state rotation $|g\rangle \rightarrow \cos(\Omega_{gf}t)|g\rangle + \sin(\Omega_{gf}t)|f\rangle$, which shows that the pulse with a duration $\frac{\pi}{2\Omega_{gf}}$ results in $|g\rangle \rightarrow |f\rangle$. As a consequence, the state (18) becomes

$$\frac{1}{\sqrt{2}}(|f\rangle|e\rangle + |e\rangle|f\rangle)|0\rangle_1|0\rangle_2|0\rangle_3|0\rangle_4. \quad (20)$$

Here and below, we assume $\Omega_{gf}, \Omega_{ge} \gg g$ so that the interaction between the qutrits and the cavities is negligible during the application of the pulses.

The double NOON states are generated through the following N steps of operation:

Step 1: Let qutrit L (R) interact with the two cavities 1 and 2 (3 and 4) [Fig. 2(a)]. Based on Eqs. (11, 12, 14, 15), one can see that after an interaction time $t_1 = \pi/(2\lambda)$, the state (20) becomes

$$\frac{1}{\sqrt{2}}(|g\rangle|e\rangle|1\rangle_1|1\rangle_2|0\rangle_3|0\rangle_4 + |e\rangle|g\rangle|0\rangle_1|0\rangle_2|1\rangle_3|1\rangle_4), \quad (21)$$

where a common phase factor i is dropped off. Then, apply a classical pulse of $\{\omega_{gf}, \frac{\pi}{2\Omega_{gf}}, -\frac{\pi}{2}\}$ to the qutrits [Fig. 2(b)], resulting in the $|g\rangle \rightarrow |f\rangle$ for each qutrit. Thus, after the pulse, the state (21) changes to

$$\frac{1}{\sqrt{2}}(|f\rangle|e\rangle|1\rangle_1|1\rangle_2|0\rangle_3|0\rangle_4 + |e\rangle|f\rangle|0\rangle_1|0\rangle_2|1\rangle_3|1\rangle_4). \quad (22)$$

Step j ($j = 2, 3, \dots, N-1$): Repeat the manipulation of step 1 [Fig. 2(a), Fig. 2(b)]. The time for each qutrit interacting with its two cavities is $t_j = \pi/(2j\lambda)$ (i.e., half a Rabi oscillation). According to Eq. (11) and Eq. (14), one can find that after an interaction time t_j , the state $|f\rangle_L|j-1\rangle_1|j-1\rangle_2$ ($|f\rangle_R|j-1\rangle_3|j-1\rangle_4$) changes to $i e^{ij\lambda t_j} |g\rangle_L|j\rangle_1|j\rangle_2$ ($i e^{ij\lambda t_j} |g\rangle_R|j\rangle_3|j\rangle_4$) which further turns into $i e^{ij\lambda t_j} |f\rangle_L|j\rangle_1|j\rangle_2$ ($i e^{ij\lambda t_j} |f\rangle_R|j\rangle_3|j\rangle_4$) due to a microwave pulse of $\{\omega_{gf}, \frac{\pi}{2\Omega_{gf}}, -\frac{\pi}{2}\}$ pumping the state $|g\rangle$ back to $|f\rangle$. Meanwhile, according to Eq. (12) and Eq. (15), both of the states $|e\rangle_L|0\rangle_3|0\rangle_4$ ($|e\rangle_R|0\rangle_1|0\rangle_2$) change to $e^{-i\lambda t_j} |e\rangle_L|0\rangle_3|0\rangle_4$ ($e^{-i\lambda t_j} |e\rangle_R|0\rangle_1|0\rangle_2$). Hence, one can easily verify that after the operation of steps (2, 3, ..., $N-1$), the state (22) changes to

$$\frac{1}{\sqrt{2}}(|f\rangle|e\rangle|N-1\rangle_1|N-1\rangle_2|0\rangle_3|0\rangle_4 + |e\rangle|f\rangle|0\rangle_1|0\rangle_2|N-1\rangle_3|N-1\rangle_4), \quad (23)$$

where a common phase factor $i^{N-2}e^{i\varphi}$ with $\varphi = \lambda \sum_{j=2}^{N-1} (j-1)t_j$ is dropped off.

Step N : Apply a classical pulse $\{\omega_{ge}, \frac{\pi}{2\Omega_{ge}}, \frac{\pi}{2}\}$ to each qutrit [Fig. 2(c)]. The interaction Hamiltonian is

$$H_{I,3} = \sum_{j=L,R} (\Omega_{ge} e^{-i\pi/2} \sigma_{ge,j}^+ + h.c.). \quad (24)$$

It is easy to show that under this Hamiltonian, the applied pulses lead to the transformation $|e\rangle \rightarrow |g\rangle$ for each qutrit. Thus, the state (23) becomes

$$\frac{1}{\sqrt{2}} (|f\rangle|g\rangle|N-1\rangle_1|N-1\rangle_2|0\rangle_3|0\rangle_4 + |g\rangle|f\rangle|0\rangle_1|0\rangle_2|N-1\rangle_3|N-1\rangle_4), \quad (25)$$

Meanwhile, let qutrit L (R) interact with the two cavities 1 and 2 (3 and 4) [Fig. 2(a)]. According to Eq. (11) and Eq. (14), one can see that after an interaction time $t_N = \pi/(2N\lambda)$, the state (25) changes to

$$\frac{1}{\sqrt{2}} (|N\rangle_1|N\rangle_2|0\rangle_3|0\rangle_4 + |0\rangle_1|0\rangle_2|N\rangle_3|N\rangle_4) |g\rangle |g\rangle, \quad (26)$$

where a common phase factor $ie^{i(N-1)\lambda t}$ is dropped off.

Eq. (26) shows that the four cavities (1, 2, 3, 4) are prepared in a double NOON state and disentangled from the qutrits. The level spacings of the qutrits need to be adjusted back to the original configuration after the operation, so that each qutrit is decoupled from their own two cavities and the central cavity, and thus the prepared double NOON state (26) remains unchanged.

The above description shows that no adjustment of the cavity frequencies is needed during the entire operation. The double-NOON-state generation utilizes classical pulses with only two different frequencies (i.e., $\omega = \omega_{gf}, \omega_{ge}$), which are readily achieved in experiments. Moreover, no measurement on the states of the coupler qutrits or the cavities is required.

The total operational time (including the initial preparation for the Bell state) is given by

$$t_{op} = \frac{\pi}{2\sqrt{2}\mu} + \sum_{j=1}^N \frac{\pi\delta}{2jg^2} + \frac{N\pi}{2\Omega_{gf}} + \frac{\pi}{2\Omega_{ge}} + 4t_d, \quad (27)$$

where $t_d \sim 1-3$ ns is the typical time required for adjusting the qutrit level spacings [28, 32]. To reduce decoherence from the qutrits and the cavities, the operation time t_{op} needs to be much shorter than the energy relaxation time $T_{k,1}$ and dephasing time $T_{k,2}$ of the level $|k\rangle$ ($k = f, e$). In principle, the t_{op} can be shortened by increasing the coupling constant μ , the pulse Rabi frequency Ω_{gf} and Ω_{ge} , and by rapidly adjusting the level spacings of the qutrits.

For cavity k ($k = 1, 2, 3, 4$), the lifetime of the cavity mode is given by $T_{cav}^k = (Q_k/\omega_k)/\bar{n}_k$, where Q_k , ω_k and \bar{n}_k are the (loaded) quality factor, frequency, and the average photon number of cavity k , respectively. For the four cavities here, the lifetime of entanglement of the cavity modes is given by

$$T_{cav} = \frac{1}{4} \min \{T_{cav}^1, T_{cav}^2, T_{cav}^3, T_{cav}^4\}, \quad (28)$$

which should be much longer than t_{op} , such that the effect of cavity decay is negligible during the operation. It is noted that decoherence from the central cavity can be neglected because the photon was populated in the central cavity for a very short time. In principle, the $T_{cav} \gg t_{op}$ can be met by choosing cavities with a high quality factor.

The inter-cavity cross coupling between the two cavities on the left (right) side is determined mostly by the coupling capacitances c_1 and c_2 (c_3 and c_4) as well as the qutrit's self capacitance C_q , because the field leakage through space is extremely low for high- Q resonators as long as the inter-cavity distance is much greater than transverse dimension of the cavities - a condition easily met in experiments for the two resonators [39]. As our numerical simulation shows below [see Fig. 4(a)], the operational fidelity is insensitive to the crosstalk of cavities 1 and 2, when the detuning between the frequencies of cavities 1 and 2 is much larger than the inter-cavity coupling constant g_{12} between cavities 1 and 2. The same holds for cavities 3 and 4). It is noted that the inter-cavity crosstalk between the side cavities and the central cavity can be neglected by adjusting the central cavity frequency such that the central cavity frequency is highly detuned from the side-cavity frequencies.

V. POSSIBLE EXPERIMENTAL IMPLEMENTATION

In this section, we discuss the fidelity for generating double NOON states with photon number $N \leq 10$. In the numerical calculations, the preparing of the initial Bell state will not be considered, since it is extremely fast due to using the resonant interaction only.

We will consider inter-cavity crosstalks of cavities on both sides, which can be described as $\varepsilon = g_{12} (e^{i\Delta t} a_1 a_2^\dagger + h.c.) + g_{34} (e^{i\Delta t} a_3 a_4^\dagger + h.c.)$, where g_{12} (g_{34}) is the coupling strength of cavities 1 and 2 (3 and 4), and we have assumed the detuning between cavity frequencies ω_{c_1} and ω_{c_2} (ω_{c_3} and ω_{c_4}) $\Delta = \omega_{c_2} - \omega_{c_1} = \omega_{c_4} - \omega_{c_3}$ for simplicity. We will also consider the unwanted qutrit-cavity interactions and inter-cavity crosstalks during the application of pulses. So the Hamiltonians $H_{I,1}$, $H_{I,2}$, and $H_{I,3}$ adopted in the double NOON state generation should be modified to $\tilde{H}_{I,1} = H_{I,1} + \varepsilon$, $\tilde{H}_{I,2} = H_{I,2} + \tilde{H}_{I,1}$, and $\tilde{H}_{I,3} = H_{I,3} + \tilde{H}_{I,1}$, respectively.

By considering dissipation and dephasing, the evolving of the system is determined by the master equation

$$\begin{aligned} \frac{d\rho}{dt} = & -i \left[\tilde{H}_{I,k}, \rho \right] + \sum_{l=1}^4 \kappa_{a_l} \mathcal{L} [a_l] \\ & + \sum_{j=L,R} \gamma_{ef,j} \mathcal{L} [\sigma_{ef,j}^-] + \gamma_{gf,j} \mathcal{L} [\sigma_{gf,j}^-] + \gamma_{ge,j} \mathcal{L} [\sigma_{ge,j}^-] \\ & + \sum_{j=L,R} \gamma_{f\varphi,j} (\sigma_{ff,j} \rho \sigma_{ff,j} - \sigma_{ff,j} \rho / 2 - \rho \sigma_{ff,j} / 2) \\ & + \sum_{j=L,R} \gamma_{e\varphi,j} (\sigma_{ee,j} \rho \sigma_{ee,j} - \sigma_{ee,j} \rho / 2 - \rho \sigma_{ee,j} / 2), \end{aligned} \quad (29)$$

where $\tilde{H}_{I,k}$ (with $k = 1, 2, 3$) are the modified $\tilde{H}_{I,1}$, $\tilde{H}_{I,2}$, and $\tilde{H}_{I,3}$, $\mathcal{L}[\Lambda] = \Lambda \rho \Lambda^\dagger - \Lambda^\dagger \Lambda \rho / 2 - \rho \Lambda^\dagger \Lambda / 2$ (with $\Lambda = a_l, \sigma_{ef,j}^-, \sigma_{gf,j}^-, \sigma_{ge,j}^-$), $\sigma_{ef,j}^- = |e\rangle_j \langle f|$, $\sigma_{gf,j}^- = |g\rangle_j \langle f|$, $\sigma_{ge,j}^- = |g\rangle_j \langle e|$, $\sigma_{ff,j} = |f\rangle_j \langle f|$, and $\sigma_{ee,j} = |e\rangle_j \langle e|$; κ_{a_l} is the decay rate of cavity l ($l = 1, 2, 3, 4$); $\gamma_{ef,j}$ ($\gamma_{gf,j}$) is the energy relaxation rate for the level $|f\rangle$ associated with the decay path $|f\rangle \rightarrow |e\rangle$ ($|f\rangle \rightarrow |g\rangle$) of qutrit j ; $\gamma_{ge,j}$ is the energy relaxation rate of the level $|e\rangle$; and $\gamma_{f\varphi,j}$ ($\gamma_{e\varphi,j}$) is the dephasing rate of the level $|f\rangle$ ($|e\rangle$) of qutrit j ($j = L, R$). The fidelity of the whole operation is given by $\mathcal{F} = \sqrt{\langle \psi_{id} | \rho | \psi_{id} \rangle}$, where $|\psi_{id}\rangle$ is the ideal output state given in Eq. (26), while ρ is the final density matrix obtained by numerically solving the master equation. For numerical calculations, we here use the QUTIP software [40, 41], which is an open-source software for simulating the dynamics of open quantum systems.

We now numerically calculate the fidelity. For flux qutrits, the transition frequency between two neighbor levels can be made to be 1–20 GHz. As an example, we choose the frequencies of qutrits as $\omega_{ef}/2\pi \sim 7.5$ GHz and $\omega_{ge}/2\pi \sim 5.0$ GHz, and the detuning $\delta/2\pi = 1.0$ GHz. As a result, we have $\omega_{c_1}/2\pi, \omega_{c_3}/2\pi \sim 4.0$ GHz, and $\omega_{c_2}/2\pi, \omega_{c_4}/2\pi \sim 8.5$ GHz, and thus $\Delta/2\pi \sim 4.5$ GHz. For simplicity, we set $\Omega_{ge} = \Omega_{gf} = \Omega$, which can be readily achieved by adjusting the pulse intensity. Other parameters used in the numerical simulations are: (i) $\gamma_{ef,j}^{-1} = 5 \mu\text{s}$, $\gamma_{gf,j}^{-1} = 5 \mu\text{s}$; (ii) $\gamma_{ge,j}^{-1} = 10 \mu\text{s}$, $\gamma_{ef,j}^{-1} = 5 \mu\text{s}$, $\gamma_{gf,j}^{-1} = 20 \mu\text{s}$ [34–38], and (iii) $\kappa_{a_l}^{-1} = 20 \mu\text{s}$ ($l = 1, 2, 3, 4$). For the cavity frequencies and $\kappa_{a_l}^{-1}$ used here, the required quality factors for the four cavities are $Q_1 = Q_3 \sim 5.0 \times 10^5$ and $Q_2 = Q_4 \sim 1.0 \times 10^6$, which are readily available in experiments [42, 43].

In Fig. 3, fidelities versus $g/2\pi$ are plotted respectively for $N = 4, 6, 8, 10$ and $\Omega/2\pi = 100, 150, 200$ MHz [33], with $g_1 = g_2 = g$ and $g_{12} = g_{34} = 0$. For $\Omega/2\pi = 150$ MHz, the best fidelity and the corresponding optimal $g/2\pi$ are: $\{0.941, 19 \text{ MHz}\}$ ($N = 4$); $\{0.903, 19 \text{ MHz}\}$ ($N = 6$); $\{0.870, 23 \text{ MHz}\}$ ($N = 8$); $\{0.831, 23 \text{ MHz}\}$ ($N = 10$). If $\Omega/2\pi$ is increased to 200 MHz, the fidelity will be improved, as shown in Fig. 3.

To see the effect of the inter-cavity crosstalk and the parameter inhomogeneity on the fidelity, we consider: (i) $g_{12} = g_{34} = 0$, $g_{12} = g_{34} = 0.1g$, and $g_{12} = g_{34} = g$ in Fig. 4(a), (ii) $g_1 = g_2$, $g_1 = 0.95g_2$, and $g_1 = 0.9g_2$ in Fig. 4(b), and (iii) $\delta_1 = \delta_2$, $\delta_1 = \delta_2 + 2\pi \times 1 \text{ MHz}$, and $\delta_1 = \delta_2 + 2\pi \times 2 \text{ MHz}$ in Fig. 4(c). Fig. 4 is plotted for $N = 10$ and $\Omega/2\pi = 200$ MHz. Fig. 4(a) shows that the effect of the inter-cavity crosstalk on the fidelity is negligible. This is due to the large detuning between the cavity frequencies ($\Delta/2\pi \sim 4.5$ GHz), compared to g_{12} and g_{34} . Fig. 4(b) shows that compared to the homogeneous case, a small difference between g_1 and g_2 only leads to a small change of fidelity. In contrast, Fig. 4(c) shows that the fidelity decreases fast as the difference between δ_1 and δ_2 increases.

VI. CONCLUSIONS

We have presented an approach for generating the double NOON states of photons in circuit QED. We believe that this work is of interest because our work is the first to demonstrate that the double NOON states of photons can be generated in circuit QED with only $N + 2$ operational steps. The numerical simulations show that high-fidelity generation of the double NOON states with $N \leq 10$ even for the imperfect devices is feasible with present-day circuit QED technique. The double NOON states are entangled states on more parties and thus different from the traditional NOON states. Compared to the NOON states, the double NOON states may achieve the same error in phase measurement using the same number of photons while requiring much less operational steps to prepare.

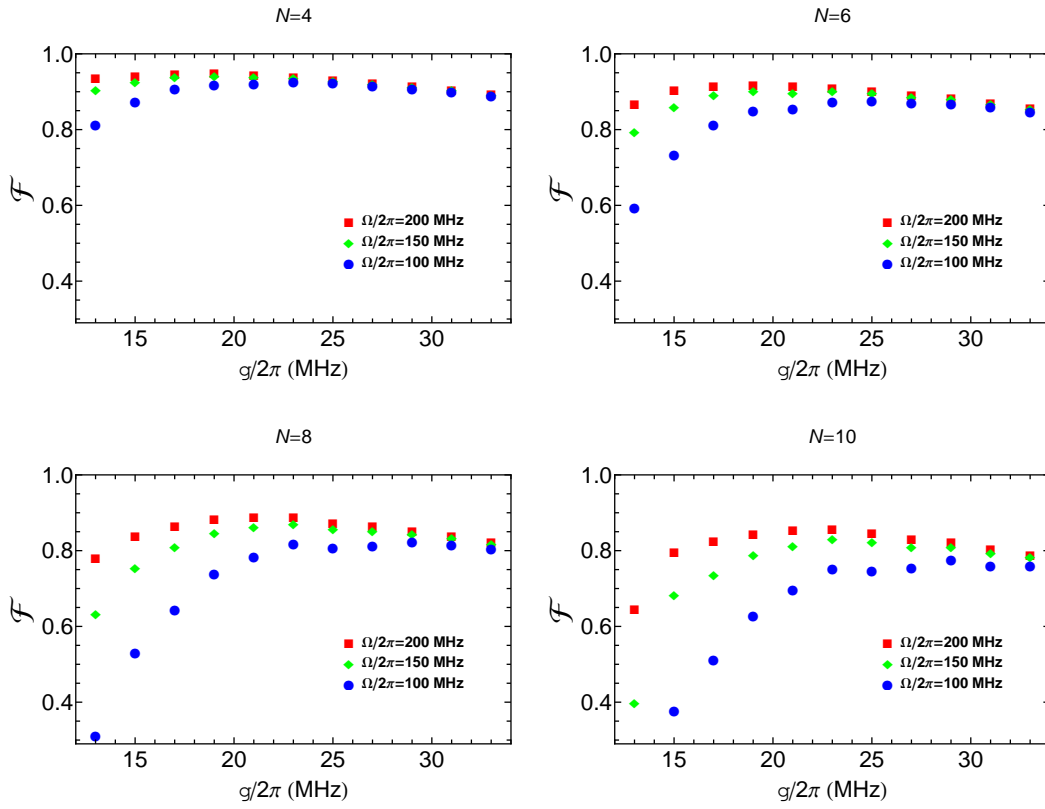


FIG. 3: (Color online) Fidelities versus $g/2\pi$ for double NOON state generation with photon numbers of $N = 4, 6, 8, 10$. For each N , $\Omega/2\pi = 100, 150, 200$ MHz [33] are considered. The figure was plotted by assuming $g_1 = g_2 = g$ and $g_{12} = g_{34} = 0$.

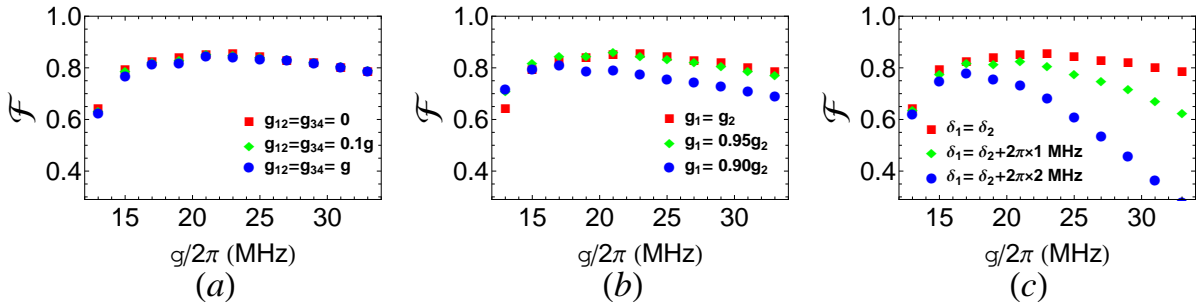


FIG. 4: (Color online) Fidelities versus $g/2\pi$ with photon numbers of $N = 10$. (a) Cases for $g_{12} = g_{34} = 0$, $g_{12} = g_{34} = 0.1g$, and $g_{12} = g_{34} = g$. (b) Cases for $g_1 = g_2$, $g_1 = 0.95g_2$, and $g_1 = 0.9g_2$ (setting $g_2 = g$). (c) Cases for $\delta_1 = \delta_2$, $\delta_1 = \delta_2 + 2\pi \times 1$ MHz, and $\delta_1 = \delta_2 + 2\pi \times 2$ MHz (setting $\delta_2 = \delta$). In (a), (b), and (c), other parameters used in the numerical simulations are the same as those used in Fig. 3.

ACKNOWLEDGMENTS

C.P. Yang and Q.P. Su were supported in part by the Ministry of Science and Technology of China under Grant No. 2016YFA0301802, the National Natural Science Foundation of China under Grant Nos 11504075, 11074062, and 11374083, and the Zhejiang Natural Science Foundation under Grant No. LZ13A040002. J.M. Liu was supported in part by the National Natural Science Foundation of China under Grant Nos 11174081 and 11134003, the National Basic Research Program of China under Grant No. 2012CB821302, and the Natural Science Foundation of Shanghai under Grant No. 16ZR1448300. This work was also supported by the funds from Hangzhou City for the Hangzhou-City Quantum Information and Quantum Optics Innovation Research Team.

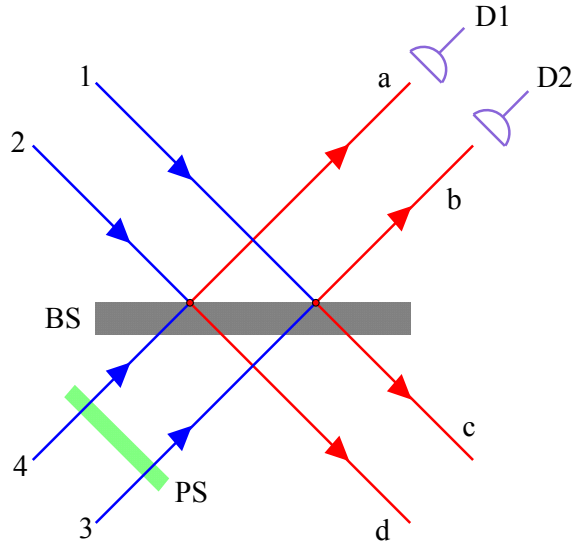


FIG. 5: (Color online) Setup for phase measurement by using a double NOON states. Initially, photons in four modes (1, 2, 3, 4) are in a double NOON state $(|NN00\rangle_{1234} + |00NN\rangle_{1234})/\sqrt{2}$. Each Photon in mode 3 (4) experiences an extra phase shift ϕ compared to each photon in mode 1 (2), which is induced by a phase shifter (PS). Here, BS represents a beam splitter, D1 and D2 represent photon detectors. The probability for coincidence measurement of N photons at mode a and N photons at mode b is $P = \eta[1 + \cos(2N\phi)]/2$ with $0 < \eta = 2^{1-2N} < 1$ for $N \neq 0$.

APPENDIX A

Here we show how to implement the measurement of $A_{DN} = (|NN00\rangle_{1234} + |00NN\rangle_{1234})(\langle NN00|_{1234} + \langle 00NN|_{1234})/2$. A simple setup for this measurement is shown in Fig. 5. Suppose photons in four modes (1, 2, 3, 4) are initially in a double NOON state $(|NN00\rangle_{1234} + |00NN\rangle_{1234})/\sqrt{2}$. The evolution of state of photons in four modes can be expressed as follows:

$$\begin{aligned}
& \frac{1}{\sqrt{2}}(|NN00\rangle_{1234} + |00NN\rangle_{1234}) \\
&= \frac{1}{\sqrt{2N!}}[(A_1^+ A_2^+)^N + (A_3^+ A_4^+)^N] \cdot |0\rangle \\
&\xrightarrow{PS} \frac{1}{\sqrt{2N!}}[(A_1^+ A_2^+)^N + e^{i2N\phi}(A_3^+ A_4^+)^N] \cdot |0\rangle \\
&\xrightarrow{BS} \frac{1}{2^N \sqrt{2N!}}[(A_b^+ + A_c^+)^N (A_a^+ + A_d^+)^N + e^{i2N\phi}(A_b^+ - A_c^+)^N (A_a^+ - A_d^+)^N] \cdot |0\rangle \\
&= \frac{1}{2^N \sqrt{2N!}}(1 + e^{i2N\phi})(A_a^+ A_b^+)^N \cdot |0\rangle + \dots \\
&= \frac{1}{2^N \sqrt{2}}(1 + e^{i2N\phi})|NN00\rangle_{abcd} + \dots,
\end{aligned}$$

where A_i^+ is the photon creation operator of mode i ($i = 1, 2, 3, 4, a, b, c, d$). The first term of the last line indicates that the probability of coincidence measurement of N photons in mode a and N photons at mode b is $P = \eta[1 + \cos(2N\phi)]/2$, which is just the expectation of A_{DN} times an additional constant $\eta = 2^{1-2N}$. Note that the appearance of η here does not affect the error of phase measurement $\Delta\phi$.

-
- [1] J. Q. You and F. Nori, “Superconducting circuits and quantum information”, Phys. Today **58**(11), 42 (2005).
[2] J. Q. You and F. Nori, “Atomic physics and quantum optics using superconducting circuits”, Nature **474**, 589 (2011).
[3] I. Buluta, S. Ashhab, and F. Nori, “Natural and artificial atoms for quantum computation”, Rep. Prog. Phys. **74**, 104401 (2011).

- [4] Z. L. Xiang, S. Ashhab, J. Q. You, and F. Nori, “Hybrid quantum circuits: Superconducting circuits interacting with other quantum systems”, *Rev. Mod. Phys.* **85**, 623 (2013).
- [5] R. Barends, J. Kelly, A. Megrant, D. Sank, E. Jeffrey, Y. Chen, Y. Yin, B. Chiaro, J. Y. Mutus, C. Neill, P. J. J. O’Malley, P. Roushan, J. Wenner, T. C. White, A. N. Cleland, and J. M. Martinis, “Coherent Josephson qubit suitable for scalable quantum integrated circuits”, *Phys. Rev. Lett.* **111**, 080502 (2013).
- [6] M. Neeley, M. Ansmann, R. C. Bialczak, M. Hofheinz, N. Katzl, E. Lucero, A. O’Connell, H. Wang, A. N. Cleland, and J. M. Martinis, “Process tomography of quantum memory in a Josephson-phase qubit coupled to a two-level state”, *Nat. Phys.* **4**, 523 (2008).
- [7] P. J. Leek, S. Filipp, P. Maurer, M. Baur, R. Bianchetti, J. M. Fink, M. Goppl, L. Steffen, and A. Wallraff, “Using sideband transitions for two-qubit operations in superconducting circuits”, *Phys. Rev. B* **79**, 180511(R) (2009).
- [8] J. D. Strand, M. Ware, F. Beaudoin, T. A. Ohki, B. R. Johnson, A. Blais, and B. L. T. Plourde, “First-order sideband transitions with flux-driven asymmetric transmon qubits”, *Phys. Rev. B* **87**, 220505(R) (2013).
- [9] J. K. Chow, J. M. Gambetta, A. D. Croles, S. T. Merkel, J. A. Smolin, C. Rigetti, S. Poletto, G. A. Keefe, M. B. Rothwell, J. R. Rozen, M. B. Ketchen, and M. Steffen, “Universal Quantum Gate Set Approaching Fault-Tolerant Thresholds with Superconducting Qubits”, *Phys. Rev. Lett.* **109**, 060501 (2012).
- [10] J. B. Chang, M. R. Vissers, A. D. Corcoles, M. Sandberg, J. Gao, D. W. Abraham, J. M. Chow, J. M. Gambetta, M. B. Rothwell, G. A. Keefe, M. Steffen, and D. P. Pappas, “Improved superconducting qubit coherence using titanium nitride”, *Appl. Phys. Lett.* **103**, 012602 (2013).
- [11] R. Barends, J. Kelly, A. Megrant, D. Sank, E. Jeffrey, Y. Chen, Y. Yin, B. Chiaro, J. Y. Mutus, C. Neill, P. J. J. O’Malley, P. Roushan, J. Wenner, T. C. White, A. N. Cleland, and J. M. Martinis, “Coherent Josephson Qubit Suitable for Scalable Quantum Integrated Circuits”, *Phys. Rev. Lett.* **111**, 080502 (2013).
- [12] J. M. Chow, J. M. Gambetta, E. Magesan, D. W. Abraham, A. W. Cross, B. R. Johnson, N. A. Masluk, C. A. Ryan, J. A. Smolin, S. J. Srinivasan, and M. Steffen, “Implementing a strand of a scalable fault-tolerant quantum computing fabric”, *Nat. Commun.* **5**, 4015 (2014).
- [13] Y. Chen, C. Neill, P. Roushan, N. Leung, M. Fang, R. Barends, J. Kelly, B. Campbell, Z. Chen, B. Chiaro, A. Dunsworth, E. Jeffrey, A. Megrant, J. Y. Mutus, P. J. J. O’Malley, C. M. Quintana, D. Sank, A. Vainsencher, J. Wenner, T. C. White, M. R. Geller, A. N. Cleland, and J. M. Martinis, “Qubit Architecture with High Coherence and Fast Tunable Coupling”, *Phys. Rev. Lett.* **113**, 220502 (2014).
- [14] M. Stern, G. Catelani, Y. Kubo, C. Grezes, A. Bienfait, D. Vion, D. Esteve, and P. Bertet, “Flux Qubits with Long Coherence Times for Hybrid Quantum Circuits”, *Phys. Rev. Lett.* **113**, 123601 (2014)
- [15] A. Wallraff, D. I. Schuster, A. Blais, L. Frunzio, R. S. Huang, J. Majer, S. Kumar, S. M. Girvin, and R. J. Schoelkopf, “Strong coupling of a single photon to a superconducting qubit using circuit quantum electrodynamics”, *Nature* **431**, 162 (2004).
- [16] T. Niemczyk, F. Deppe, H. Huebl, E. P. Menzel, F. Hocke, M. J. Schwarz, J. J. Garcia-Ripoll, D. Zueco, T. Hummer, E. Solano, A. Marx, and R. Gross, “Circuit quantum electrodynamics in the ultrastrong-coupling regime”, *Nat. Phys.* **6**, 772 (2010).
- [17] A. N. Boto, P. Kok, D. S. Abrams, S. L. Braunstein, C. P. Williams, and J. P. Dowling, “Quantum interferometric optical lithography: Exploiting entanglement to beat the diffraction limit”, *Phys. Rev. Lett.* **85**, 2733 (2000).
- [18] M. D’Angelo, M. V. Chekhova, and Y. Shih, “Two-photon Diffraction and Quantum Lithography”, *Phys. Rev. Lett.* **87**, 013602 (2001).
- [19] P. Kok, H. Lee, and J. P. Dowling, “Creation of large-photon-number path entanglement conditioned on photodetection”, *Phys. Rev. A* **65**, 052104 (2002).
- [20] M. W. Mitchell, J. S. Lundeen, and A. M. Steinberg, “Super-resolving phase measurements with a multi-photon entangled state”, *Nature* **429**, 161 (2004).
- [21] M. Muller, H. Vural, and P. Michler, “Phase super-resolution with NOON states generated by on demand single-photon sources”, arXiv:1603.00906
- [22] J. Joo, W. J. Munro, and T. P. Spiller, “Quantum metrology with entangled coherent states”, *Phys. Rev. Lett.* **107**, 083601 (2011).
- [23] C. H. Bennett and B. D. DiVincenzo, “Quantum information and computation”, *Nature* **404**, 247 (2000).
- [24] W. Heitler, “The Quantum Theory of Radiation”, 3rd ed. (Oxford University Press, London, 1954).
- [25] F. W. Strauch, K. Jacobs and R. W. Simmonds, “Arbitrary control of entanglement between two superconducting resonators”, *Phys. Rev. Lett.* **105**, 050501 (2010).
- [26] S. T. Merkel and F. K. Wilhelm, “Generation and detection of NOON states in superconducting circuits”, *New J. Phys.* **12**, 093036 (2010).
- [27] H. Wang, M. Mariantoni, R. C. Bialczak, M. Lenander, E. Lucero, M. Neeley, A. O’Connell, D. Sank, M. Weides, J. Wenner, T. Yamamoto, Y. Yin, J. Zhao, J. M. Martinis, and A. N. Cleland, “Deterministic entanglement of photons in two superconducting microwave resonators”, *Phys. Rev. Lett.* **106**, 060401 (2011).
- [28] Q. P. Su, C. P. Yang, and S. B. Zheng, “Fast and simple scheme for generating NOON states of photons in circuit QED”, *Scientific Reports* **4**, 3898 (2014).
- [29] S. J. Xiong, Z. Sun, J. M. Liu, T. Liu, and C. P. Yang, “Efficient scheme for generation of photonic NOON states in circuit QED”, *Optics Letters* **40**, 2221 (2015).
- [30] D. F. V. James, “Effective Hamiltonian theory and its applications in quantum information”, arXiv:0706.1090.
- [31] J. Clarke and F. K. Wilhelm, “Superconducting quantum bits”, *Nature* **453**, 1031 (2008).
- [32] Y. Yu and S. Han, Private communication (2015).

- [33] M. Baur, S. Filipp, R. Bianchetti, J. M. Fink, M. Gpl, L. Steffen, P. J. Leek, A. Blais, and A. Wallraff, “Measurement of Autler-Townes and mollow transitions in a strongly driven superconducting qubit”, *Phys. Rev. Lett.* **102**, 243602 (2009).
- [34] F. Yan, S. Gustavsson, A. Kamal, J. Birenbaum, A. P. Sears, D. Hover, T. J. Gudmundsen, D. Rosenberg, G. Samach, and S. Weber *et al.*, “The Flux qubit revisited to enhance coherence and reproducibility”, *Nat. Commun.* **7**, 12964 (2016).
- [35] J. Q. You, X. Hu, S. Ashhab, and F. Nori, “Low-decoherence flux qubit”, *Phys. Rev. B* **75**, 140515(R) (2007).
- [36] M. J. Peterer, S. J. Bader, X. Jin, F. Yan, A. Kamal, T. J. Gudmundsen, P. J. Leek, T. P. Orlando, W. D. Oliver, and S. Gustavsson, “Coherence and decay of higher energy levels of a superconducting transmon qubit”, *Phys. Rev. Lett.* **114**, 010501 (2015).
- [37] C. Rigetti, J. M. Gambetta, S. Poletto, B. L. T. Plourde, J. M. Chow, A. D. Córcoles, J. A. Smolin, S. T. Merkel, J. R. Rozen, and G. A. Keefe *et al.*, “Superconducting qubit in a waveguide cavity with a coherence time approaching 0.1 ms”, *Phys. Rev. B* **86**, 100506(R) (2012).
- [38] I. M. Pop, K. Geerlings, G. Catelani, R. J. Schoelkopf, L. I. Glazman, and M. H. Devoret, “Coherent suppression of electromagnetic dissipation due to superconducting quasiparticles”, *Nature* **508**, 369 (2014).
- [39] C. P. Yang, Q. P. Su, and S. Han, “Generation of Greenberger-Horne-Zeilinger entangled states of photons in multiple cavities via a superconducting qutrit or an atom through resonant interaction”, *Phys. Rev. A* **86**, 022329 (2012).
- [40] J. R. Johansson, P. D. Nation, and F. Nori, QuTiP: An opensource Python framework for the dynamics of open quantum systems, *Comput. Phys. Commun.* **183**, 1760 (2012).
- [41] J. R. Johansson, P. D. Nation, and F. Nori, QuTiP 2: A Python framework for the dynamics of open quantum systems, *Comput. Phys. Commun.* **184**, 1234 (2013).
- [42] W. Chen, D. A. Bennett, V. Patel, and J. E. Lukens, “Substrate and process dependent losses in superconducting thin film resonators”, *Sci. Technol.* **21**, 075013 (2008).
- [43] P. J. Leek, M. Baur, J. M. Fink, R. Bianchetti, L. Steffen, S. Filipp, and A. Wallraff, “Cavity quantum electrodynamics with separate photon storage and qubit readout modes”, *Phys. Rev. Lett.* **104**, 100504 (2010).